Importance of group X–secreted phospholipase A_2 in allergen-induced airway inflammation and remodeling in a mouse asthma model

William R. Henderson Jr.,[1] Emil Y. Chi,[2] James G. Bollinger,[3] Ying-tzang Tien,[2] Xin Ye,[1] Luca Castelli,[5] Yuri P. Rubtsov,[5] Alan G. Singer,[3] Gertrude K.S. Chiang,[1] Timo Nevalainen,[7] Alexander Y. Rudensky,[5,6] and Michael H. Gelb[3,4]

[1]Center for Allergy and Inflammation, Department of Medicine, University of Washington, Seattle, WA 98109
[2]Department of Pathology, [3]Department of Chemistry, [4]Department of Biochemistry, [5]Department of Immunology, and [6]Howard Hughes Medical Institute, University of Washington, Seattle, WA 98195
[7]Department of Pathology, University of Turku and Turku University Hospital, 20520 Turku, Finland

Arachidonic acid metabolites, the eicosanoids, are key mediators of allergen-induced airway inflammation and remodeling in asthma. The availability of free arachidonate in cells for subsequent eicosanoid biosynthesis is controlled by phospholipase A_2s (PLA_2s), most notably cytosolic PLA_2-α. 10 secreted PLA_2s ($sPLA_2$s) have also been identified, but their function in eicosanoid generation is poorly understood. We investigated the role of group X $sPLA_2$ ($sPLA_2$-X), the $sPLA_2$ with the highest in vitro cellular phospholipolysis activity, in acute and chronic mouse asthma models in vivo. The lungs of $sPLA_2$-$X^{-/-}$ mice, compared with those of $sPLA_2$-$X^{+/+}$ littermates, had significant reduction in ovalbumin-induced infiltration by $CD4^+$ and $CD8^+$ T cells and eosinophils, goblet cell metaplasia, smooth muscle cell layer thickening, subepithelial fibrosis, and levels of T helper type 2 cell cytokines and eicosanoids. These data direct attention to $sPLA_2$-X as a novel therapeutic target for asthma.

CORRESPONDENCE
William R. Henderson Jr.:
joangb@u.washington.edu
OR
Michael H. Gelb:
gelb@chem.washington.edu

Abbreviations used: BAL, bronchoalveolar lavage; cysLT, cysteinyl leukotriene; $cPLA_2$-α, cytosolic group IVA PLA_2; EIA, enzyme immunoassay; i.n., intranasal; LTB_4, LTC_4, LTD_4, and LTE_4, leukotriene B_4, C_4, D_4, and E_4, respectively; MOX, methoxime; PAS, periodic acid Schiff; PGD_2 and PGE_2, prostaglandin D_2 and E_2, respectively; PLA_2, phospholipase A_2; R_L, lung resistance; RT, real time; $sPLA_2$, secreted PLA_2; $sPLA_2$-X, group X $sPLA_2$.

Allergen-induced airway inflammation in asthma is characterized by eosinophil and $CD4^+$ and $CD8^+$ T cell infiltration of the airways and accompanied by airway structural changes (i.e., airway remodeling), including goblet cell metaplasia, increased smooth muscle mass, and subepithelial fibrosis from excessive deposition of extracellular matrix components such as collagen and laminin (for review see references 1, 2). Leukotrienes and prostaglandins are, respectively, 5-lipoxygenase and cyclooxygenase metabolites of arachidonic acid (i.e., eicosanoids) that are important in the pathogenesis of asthma. Release of 5-lipoxygenase products leukotriene B_4 (LTB_4), the cysteinyl leukotrienes (cysLTs) C_4, D_4, and E_4, and cyclooxygenase products prostaglandin D_2 (PGD_2) and thromboxane A_2 from inflamed airways leads to airway hyperresponsiveness and airflow obstruction with mucus glycoproteins. Evidence from animal models and patients with asthma suggest that these eicosanoids are key molecules that promote airway inflammation as potent chemoattractants for eosinophils, T cells, and other inflammatory cells; cause plasma extravasation and edema; modulate airway smooth muscle cell function; and induce release of extracellular matrix components (3–5).

The availability of free arachidonate in cells and, thus, the biosynthesis of leukotrienes and other eicosanoids, including prostaglandins, is tightly controlled by the regulated action of phospholipase A_2s (PLA_2s) that release this fatty acid by hydrolysis of the *sn*-2 ester of glycerophospholipids present as major components of cell membranes. Mammalian cells contain multiple types of PLA_2s (6), but it is generally accepted that cytosolic group IVA PLA_2-α ($cPLA_2$-α; also known as group IVA PLA_2; *PLA2G4A*) plays a pivotal role in agonist-mediated arachidonate release for the biosynthesis of the eicosanoids. This is based on studies

The online version of this article contains supplemental material.

with cPLA$_2$-α inhibitors (7–10) and cPLA$_2$-α–deficient mice (11–13). The mammalian genome also encodes 10 secreted PLA$_2$s (sPLA$_2$s). The role of these enzymes in eicosanoid biosynthesis is much less clear. Disruption of the group V sPLA$_2$ gene (*PLA2G5*) in mice leads to ~50% reduction in the amount of LTC_4 and PGE_2 production in zymosan-stimulated peritoneal macrophages (14). Group IIA, V, and X sPLA$_2$s have been shown to coordinate with cPLA$_2$-α to augment arachidonate release from cultured cells (15–20), but the mechanism for this coordinate action between cPLA$_2$-α and sPLA$_2$ is not known.

A systematic investigation of the interfacial kinetic and binding properties of the full set of mouse and human sPLA$_2$s shows that the group X sPLA$_2$ (sPLA$_2$-X; *PLA2G10*) stands out as having the highest phospholipolysis activity when added to cultured cells (21, 22). Based on these findings and the fact that sPLA$_2$-X is expressed in human (23, 24) and mouse lungs (this study), we investigated the possible role of sPLA$_2$-X in a mouse asthma model by generating a sPLA$_2$-X–deficient mouse for studies of allergen-induced airway inflammation and remodeling. In this initial study, we explored an animal disease model rather than experiments with single cell types in vitro, because sPLA$_2$-X is a secreted enzyme and can potently act extracellularly on many, if not all, mammalian cell types to liberate arachidonic acid. Therefore, studies with cultured mammalian cells cannot shed sufficient light on the behavior of sPLA$_2$-X in tissues. This is a different situation than with cPLA$_2$-α that acts in the cytoplasm.

RESULTS

Generation and characterization of the sPLA$_2$-X$^{-/-}$ mouse

Mutation of the mouse sPLA$_2$-X gene was accomplished by retroviral-mediated insertion of an exon-trapping cassette (see Materials and methods). DNA sequence analysis revealed that the trapping cassette is located in the intron between exons 3 and 4 of the sPLA$_2$-X gene. Real-time (RT)–PCR analysis using primers hybridizing to exons 2 and 4 and cDNA made from mouse testis, colon, and stomach revealed ~1,000-fold reduction in sPLA$_2$-X mRNA levels in the sPLA$_2$-X$^{-/-}$ mouse versus the wild-type littermate. We also looked for sPLA$_2$-X protein in stomach extracts using a sensitive time-resolved fluorescence immunoassay (25). When 24 μg of stomach lysate protein was analyzed from a sPLA$_2$-X$^{+/+}$ mouse, 0.2 ng sPLA$_2$-X protein was detected, whereas no sPLA$_2$-X protein was detected when 34 μg of lysate protein from a sPLA$_2$-X$^{-/-}$ mouse was used.

Allergen-induced airway inflammation and expression of sPLA$_2$-X

Important insights into the mechanisms of chronic inflammation and remodeling in asthma have come from animal models that reproduce key morphologic and physiologic features of human asthma. To study the in vivo effects of sPLA$_2$ deficiency on the asthma phenotype, we used OVA as a model allergen to induce allergen-specific pulmonary disease in wild-type and sPLA$_2$-X$^{-/-}$ mice. In the acute asthma protocol (3), OVA-sensitized mice challenged with four doses of OVA display, by day 29, a disease strikingly similar to allergen-induced human asthma, including (a) circulating levels of allergen-specific IgE; (b) a marked influx of eosinophils and T cells into the airways; (c) increased levels of mucus glycoproteins, Th2 cell cytokines (IL-4, IL-5, and IL-13), and leukotrienes and other eicosanoids in bronchoalveolar lavage (BAL) fluid; and (d) pulmonary hyperreactivity to methacholine compared with saline-treated control mice. When the intranasal (i.n.) OVA challenges are continued periodically in the chronic asthma protocol (4, 26), by day 76 the mice have striking features of airway remodeling, including (a) goblet cell metaplasia, (b) increased smooth muscle cell layer

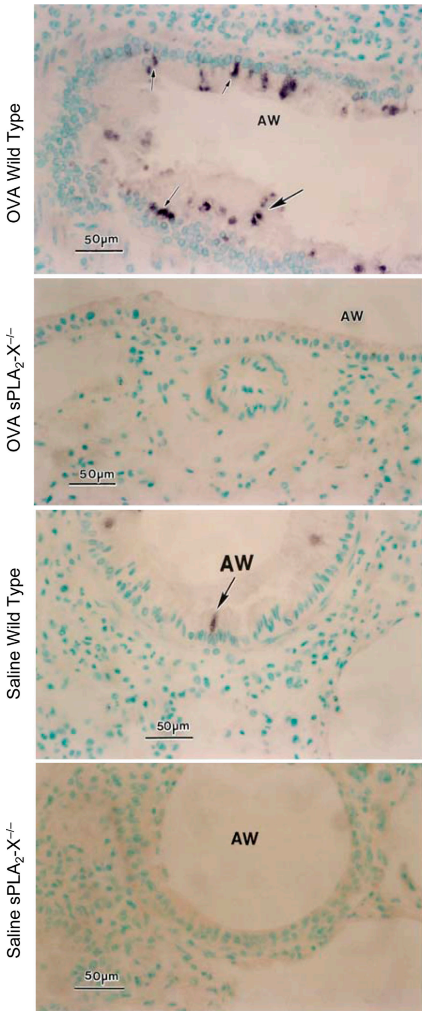

Figure 1. Absent sPLA$_2$-X expression in lungs of sPLA$_2$-X$^{-/-}$ mice. Lung tissue was obtained on day 29 (acute asthma model) from sPLA$_2$-X$^{+/+}$ and sPLA$_2$-X$^{-/-}$ mice treated with either OVA or saline and examined by immunocytochemistry for sPLA$_2$-X expression. Arrows indicate peroxidase-positive cells in the airways (AW) expressing sPLA$_2$-X. Additional airway sections of OVA-treated sPLA$_2$-X$^{+/+}$ mice are shown in Fig. S1. Absent sPLA$_2$-X expression in the splenic tissue of sPLA$_2$-X$^{-/-}$ mice is shown in Fig. S2. Bars, 50 μm.

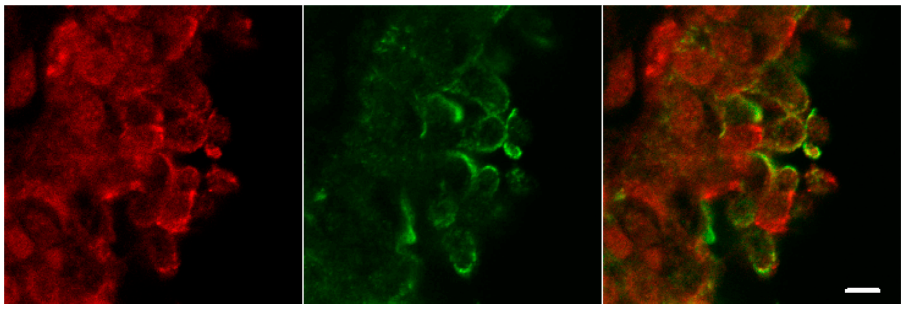

Figure 2. Colocalization of sPLA$_2$-X with airway epithelial cells expressing mucin 5AC glycoprotein in OVA-treated wild-type mice. Red fluorophore (Alexa Fluor 594) localization of sPLA$_2$-X (left), green fluorophore (Alexa Fluor 488) localization of mucin 5AC (middle), and colocalization of sPLA$_2$-X with mucin 5AC–positive airway epithelial cells (right). Bar, 20 μm.

mass, and (c) extensive subepithelial collagen deposition and airway wall thickening.

sPLA$_2$-X expression in the lungs and the spleen of sPLA$_2$-X$^{-/-}$ and wild-type mice in the acute asthma model was examined by immunocytochemistry. sPLA$_2$-X was expressed in the airway epithelium in the lungs in saline-treated wild-type mice but not in sPLA$_2$-X$^{-/-}$ mice (Fig. 1). After OVA sensitization and challenge, sPLA$_2$-X expression greatly increased in the columnar cells lining the airways of wild-type mice but remained undetected in sPLA$_2$-X$^{-/-}$ mice (Fig. 1 and Fig. S1, available at http://www.jem.org/cgi/content/full/jem.20070029/DC1). Confocal immunofluorescence microscopy demonstrated colocalization of sPLA$_2$-X with airway epithelial cells expressing mucin 5AC glycoprotein (Fig. 2). Macrophages contributed to sPLA$_2$-X expression in the airways, because alveolar macrophages, isolated from BAL fluid cells of OVA-treated wild-type mice (but not sPLA$_2$-X$^{-/-}$ mice), exhibited strong reactivity for sPLA$_2$-X by immunocytochemistry (Fig. 3). Splenic mononuclear cells also expressed sPLA$_2$-X in sPLA$_2$-X$^{+/+}$ mice but not in sPLA-X$^{-/-}$ mice (Fig. S2). No staining reaction for sPLA$_2$-X was observed when immunocytochemistry was performed with preimmune serum (Fig. S2).

Effect of sPLA$_2$-X deficiency on allergen-induced recruitment of inflammatory cells into the lungs and hyperresponsiveness

On day 29, 24 h after the final i.n. OVA challenge in animals from each experimental group (i.e., acute asthma model), the effect of sPLA$_2$-X deficiency on allergen-induced airway inflammation and hyperreactivity was determined. OVA-treated sPLA$_2$-X$^{+/+}$ mice had a sixfold increase in total cells recovered in BAL fluid compared with the saline group control (Fig. 4 a); ~50% of the BAL fluid cells were eosinophils in the OVA-treated sPLA$_2$-X$^{+/+}$ mice. The total number of inflammatory cells and eosinophils in the BAL fluid of OVA-treated sPLA$_2$-X$^{-/-}$ mice was significantly reduced compared with wild-type controls (Fig. 4 a). By light microscopy and morphometry, an influx of eosinophils and mononuclear cells into the lungs around the airways and blood vessels, airway goblet cell metaplasia/mucus hypersecretion, and interstitial edema were observed in OVA-treated sPLA$_2$-X$^{+/+}$ mice compared with saline controls (Fig. 4, b and c; and Fig. S3, available at http://www.jem.org/cgi/content/full/jem.20070029/DC1). This increased infiltration of total inflammatory cells and eosinophils, goblet cell metaplasia/mucus hypersecretion, and edema of the airway interstitium were markedly decreased in OVA-treated sPLA$_2$-X$^{-/-}$ mice compared with sPLA$_2$-X$^{+/+}$ mice (Fig. 4, b and c; and Fig. S3). Using invasive plethysmography to determine lung resistance (R_L), airway hyperreactivity to aerosolized methacholine was significantly increased in the OVA-treated wild-type mice compared with saline controls (Fig. 4 d). In contrast, pulmonary responses in the sPLA$_2$-X$^{-/-}$ mice were not significantly different between the OVA and saline treatment groups (Fig. 4 d). In vivo airway responsiveness to aerosolized methacholine was also determined on day 29 in conscious, freely moving, spontaneously breathing mice using noninvasive whole-body plethysmography, and the same trends for Penh

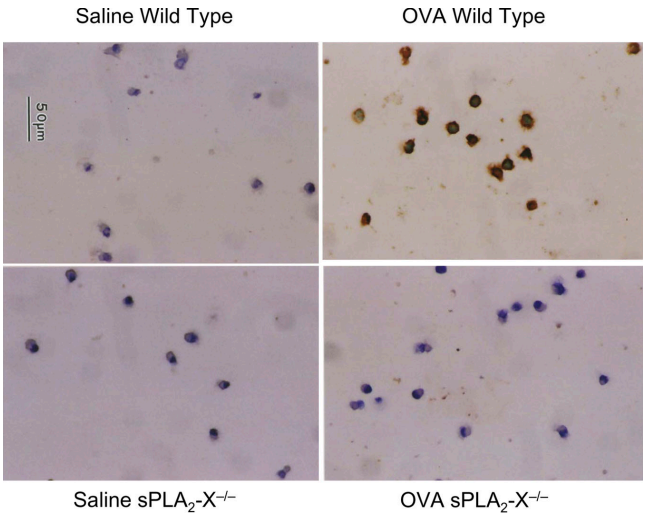

Figure 3. sPLA$_2$-X expression in alveolar macrophages of wild-type mice. Alveolar macrophages were isolated on day 29 from sPLA$_2$-X$^{+/+}$ and sPLA$_2$-X$^{-/-}$ mice treated with either OVA or saline and examined by immunocytochemistry for sPLA$_2$-X expression. Bar, 50 μm.

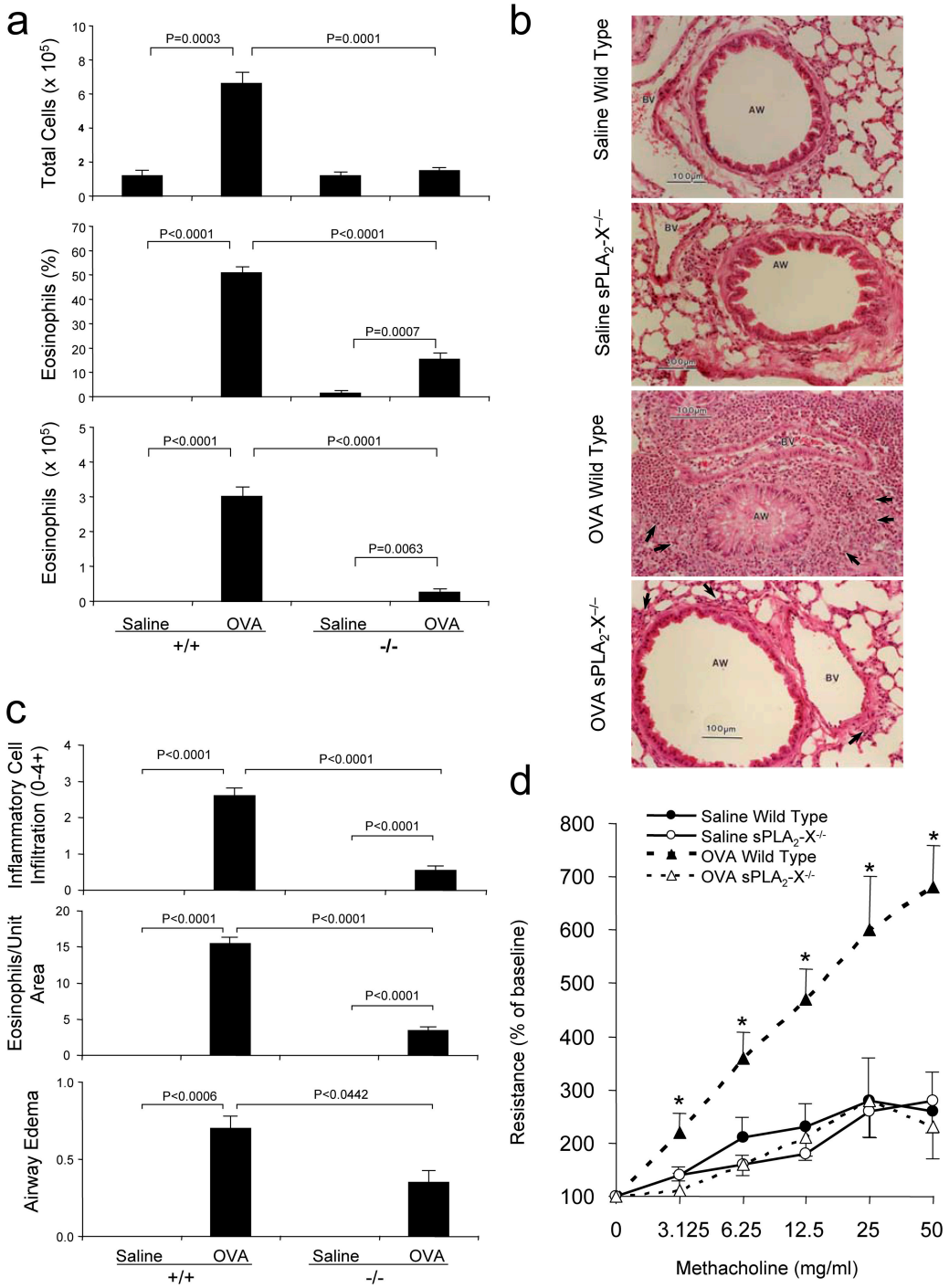

Figure 4. Impaired allergen-induced airway inflammation and hyperreactivity in sPLA$_2$-X$^{-/-}$ mice. (a) BAL fluid was obtained on day 29 from saline-treated ($n = 5$) and OVA-treated ($n = 9$) sPLA$_2$-X$^{+/+}$ mice (+/+) and saline-treated ($n = 7$) and OVA-treated ($n = 8$) sPLA$_2$-X$^{-/-}$ mice (−/−), and the number of total cells and percentage and number of eosinophils were determined. (b) Lung sections of saline- and OVA-treated sPLA$_2$-X$^{+/+}$ and sPLA$_2$-X$^{-/-}$ mice were stained with hematoxylin and eosin. Arrows indicate inflammatory cells. AW, airways; BV, blood vessels. Bars, 100 μm. (c) The intensity of the total inflammatory cell infiltrate (0–4+ scale), the number of eosinophils per unit area (2,200 μm^2), and airway edema (0–4+ scale) in the lungs on day 29 were determined by morphometric analysis. (d) Allergen-induced airway hyperresponsiveness was assessed by invasive plethysmography on day 29 in wild-type (+/+) and sPLA$_2$-X$^{-/-}$ (−/−) mice as the degree of bronchoconstriction to aerosolized methacholine (0, 3.125, 6.25, 12.5, 25, and 50 mg/ml). R_L was calculated as described in Materials and methods and is shown as the percentage of baseline response to aerosolized normal saline. *, $P < 0.05$ versus saline. Data in a, c, and d represent the mean ± SEM.

values were observed as for the invasive R_L measurements (unpublished data).

Effect of sPLA$_2$-X deficiency on allergen-induced airway remodeling

Wild-type mice challenged with OVA periodically over a 75-d period (i.e., chronic asthma model) had persistent airway infiltration by eosinophils and edema (Fig. 5 a; and Fig. S4 and Fig. S5, available at http://www.jem.org/cgi/content/full/jem.20070029/DC1), goblet cell metaplasia and mucus hypersecretion on day 76 (Fig. 5, a and b), and increased airway smooth muscle mass and collagen deposition (Fig. 6, a and b) compared with saline controls. These features of allergen-induced airway remodeling were significantly reduced in sPLA$_2$-X$^{-/-}$ mice (Fig. 5, a and b; and Fig. 6, a and b).

Effect of sPLA$_2$-X deficiency on Th2 responses

A molecular hallmark of asthma is Th2 cytokine expression. We examined the effect of sPLA$_2$-X deficiency on Th2 cell–driven OVA-specific IgE levels, trafficking of T cells to the lungs, and pulmonary Th2 versus Th1 cytokine expression in both the acute and chronic mouse asthma models. Circulating levels of allergen-specific IgE in blood were reduced on day 29 in sPLA$_2$-X$^{-/-}$ mice compared with wild-type controls after OVA treatment (Fig. 7 a). A substantial increase in the total number of T cells and also in the numbers of both CD4$^+$ and CD8$^+$ cells was seen in the BAL fluid of wild-type mice after OVA treatment on day 29 (Fig. 7 b). In contrast, negligible trafficking of T cells to the BAL fluid was observed in allergen-challenged sPLA$_2$-X$^{-/-}$ mice (Fig. 7 b). By RT-PCR, gene expression of the Th2 cytokines IL-4, IL-5, and IL-13 was markedly increased in whole-lung tissue of OVA-sensitized/challenged sPLA$_2$-X$^{+/+}$ mice compared with saline-treated controls on day 76 (Fig. 7 c). In OVA-treated sPLA$_2$-X$^{-/-}$ mice compared with wild-type controls, gene expression of IL-4, IL-5, and IL-13 was significantly reduced (Fig. 7 c). No significant change in gene expression of the Th1 cytokines IL-2 and IFN-γ, the lymphocyte-activating factor IL-1β, or the Th1-inducing cytokine IL-12 was seen in either wild-type or sPLA$_2$-X$^{-/-}$ mice after OVA treatment compared with saline controls (Fig. 7 c). Significant levels of IL-4, IL-5, and IL-13 proteins were found in the BAL fluid of OVA-treated sPLA$_2$-X$^{+/+}$ mice compared with the saline control group on day 76 (Fig. 7 d). In the BAL fluid of OVA-treated sPLA$_2$-X$^{-/-}$ mice, IL-4 was not detected, and IL-5 and IL-13 levels were significantly reduced compared with wild-type controls (Fig. 7 d). IL-1β, IL-2, IL-12 (p70), and IFN-γ were not detected in the BAL fluid of wild-type and sPLA$_2$-X$^{-/-}$ mice after either saline or OVA treatment. Similar reductions in the pulmonary Th2 cytokine responses were observed in sPLA$_2$-X$^{-/-}$ compared

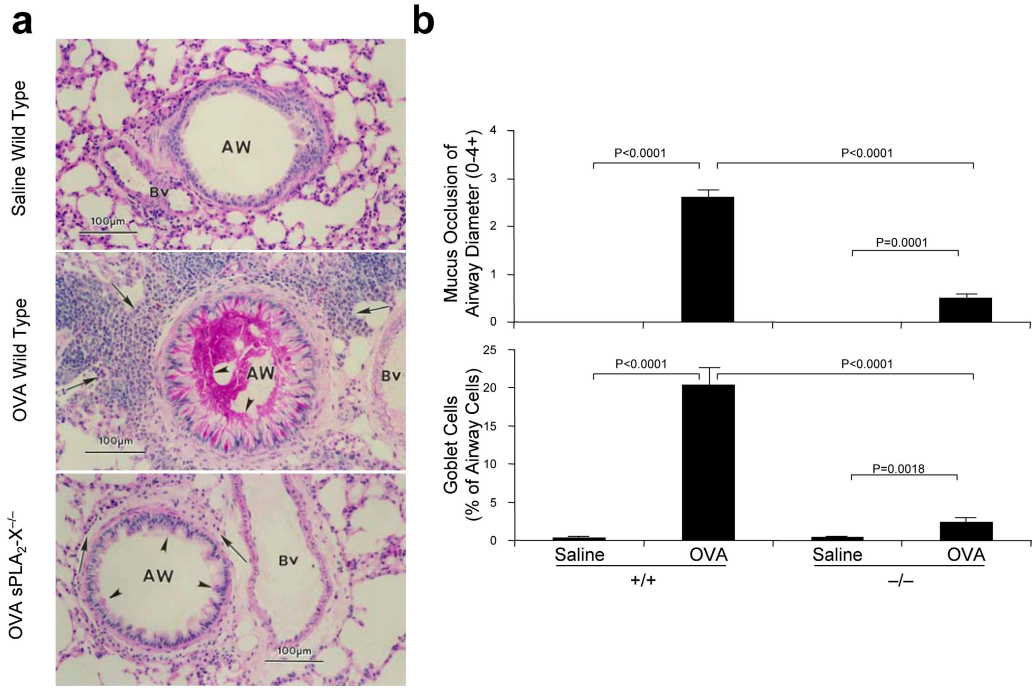

Figure 5. sPLA$_2$-X deficiency decreases allergen-induced goblet cell metaplasia. (a) Lung tissue was obtained on day 76 (chronic asthma model) from sPLA$_2$-X$^{+/+}$ and sPLA$_2$-X$^{-/-}$ mice treated with either saline or OVA and stained with alcian blue/PAS. Arrowheads indicate goblet cells, and arrows indicate inflammatory cells. AW, airways; BV, blood vessels. Bars, 100 μm. (b) The occlusion of airway diameter by mucus (0–4+ scale) and the percentage of total airway epithelial cells positive for mucus glycoproteins by alcian blue/PAS staining in the lungs were determined by morphometric analysis ($n = 4$ for each group). Impaired allergen-induced airway goblet cell metaplasia and mucus hypersecretion in sPLA$_2$-X$^{-/-}$ mice on day 29 in an acute asthma model are shown in Fig. S3. Data represent the mean ± SEM.

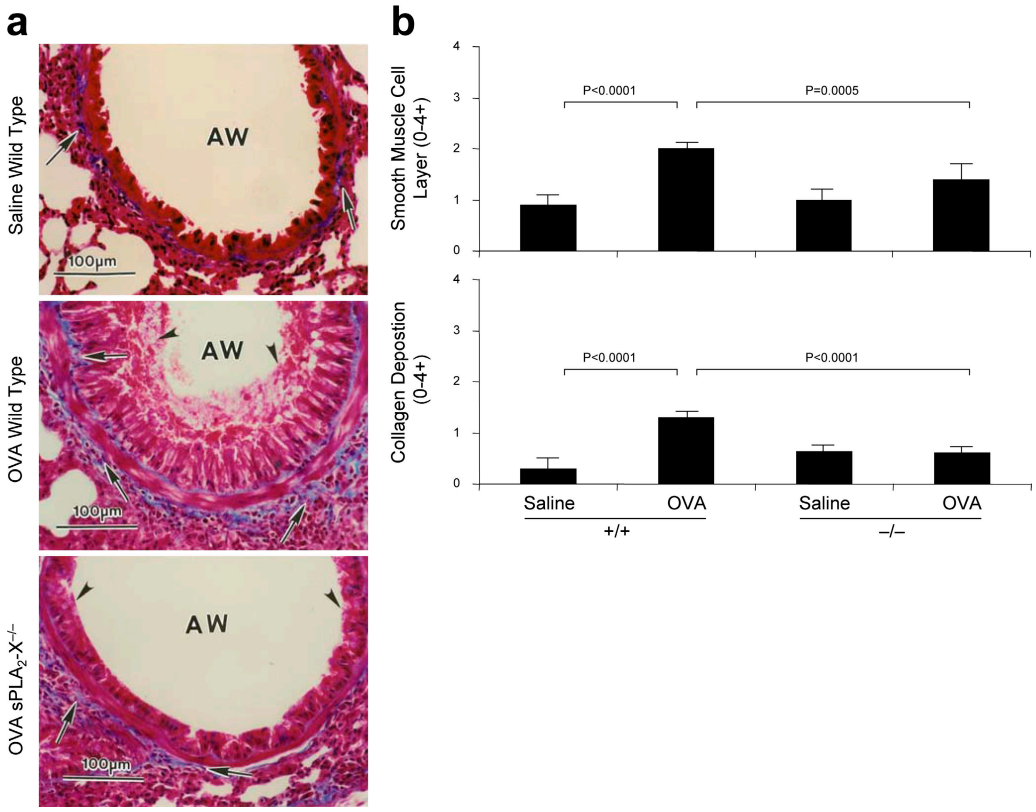

Figure 6. sPLA2-X deficiency reduces allergen-induced increased smooth muscle cell layer mass and subepithelial fibrosis. (a) Lung tissue was obtained on day 76 from $sPLA_2$-$X^{+/+}$ and $sPLA_2$-$X^{-/-}$ mice treated with either saline or OVA and stained with Masson's trichrome stain. Arrows indicate collagen and arrowheads indicate mucus. AW, airways. Bars, 100 μm. (b) Airway smooth muscle cell layer mass and subepithelial collagen deposition were determined by morphometry (0–4+ scale). Impaired allergen-induced BAL fluid eosinophilia and airway tissue inflammation on day 76 in $sPLA_2$-$X^{-/-}$ mice in a chronic asthma model are shown in Fig. S4 and Fig. S5, respectively. Data represent the mean ± SEM.

with wild-type mice in the acute asthma model (unpublished data).

To examine the effect of $sPLA_2$-X deficiency on systemic $CD4^+$ T cell–mediated production of Th2 cytokines in response to antigenic challenge, we used flow cytometric analysis to examine production of IL-4, IL-5, and IL-10, as well as the proinflammatory cytokines IFN-γ and TNF-α, upon overnight in vitro stimulation of splenic $CD4^+$ T cells from OVA-immunized and unimmunized mutant and wild-type mice in the presence of OVA. Comparable antigen-specific production of IL-5 (Fig. 8 a) and IL-10 (Fig. 8 a) was detected in both mutant and wild-type T cells, as indicated by ∼2–2.5-fold increase in the percentage of cytokine-producing $CD4^+$ T cells in the presence versus absence of OVA. In contrast to IL-5 and IL-10, antigen-specific production of IL-4, IFN-γ, and TNF-α was not detected using intracellular cytokine staining, suggesting that the frequency of OVA-specific $CD4^+$ T cells producing these cytokines was below the detection level (unpublished data). Therefore, we used a single-cell immunospot assay (ELISPOT) to measure their OVA-stimulated production of IL-4 and IFN-γ. In agreement with flow cytometric analyses of IL-5 and IL-10 production, we found no difference in their ability to produce IL-4 (Fig. 8 c) and IFN-γ (Fig. 8 d). Further, there was a comparable ability to produce IL-4 by splenic $CD4^+$ T cells from $sPLA_2$-$X^{-/-}$ mice and wild-type controls in response to anti-CD3/anti-CD28 stimulation (Fig. 8 e). Thus, $sPLA_2$-X deficiency does not result in a general repression of Th2 or Th1 cytokine production.

Effect of $sPLA_2$-X deficiency on eicosanoid release

To assess the effect of $sPLA_2$-X deficiency on arachidonic acid release, we used an acute asthma model to measure the levels of eicosanoids that are derived from this fatty acid, specifically via the cyclooxygenase pathway leading to PGD_2 and PGE_2 and via the 5-lipoxygenase pathway leading to LTB_4 and cysLTs C_4, D_4, and E_4 (i.e., total cysLTs). Because of its chemical instability (27), PGD_2 was converted to a stable methoxime (MOX) derivative to prevent its further chemical degradation, and PGD_2-MOX was assayed to determine PGD_2 levels. Because PGE_2 is rapidly and extensively metabolized in vivo (28), both native PGE_2 and its 13,14-dihydro-15-keto metabolite were assayed to determine the total PGE_2 levels produced. In an acute asthma

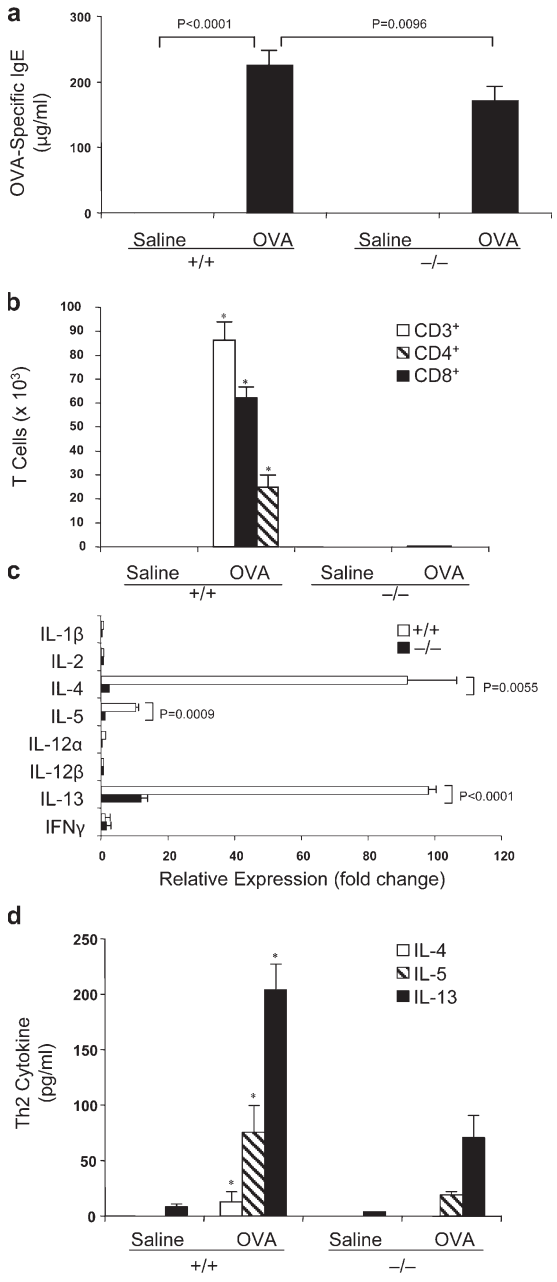

Figure 7. Impaired Th2 cytokine responses in sPLA$_2$-X$^{-/-}$ mice. (a) OVA-specific IgE levels were determined in plasma obtained on day 29 from saline- and OVA-treated mGX$^{+/+}$ (+/+) and sPLA$_2$-X$^{-/-}$ (−/−) mice. (b) The number of CD3$^+$, CD4$^+$, and CD8$^+$ T cells in the BAL fluid on day 29 was determined by flow cytometry. Low cell levels ($\times 10^3$) not shown on the graph are as follows: saline-treated wild-type mice (CD3$^+$, 0.111 ± 0.001; CD4$^+$, 0.083 ± 0.002; and CD8$^+$, 0.028 ± 0.002 [reference 1]); saline-treated sPLA$_2$-X$^{-/-}$ mice (CD3$^+$, 0.103 ± 0.002; CD4$^+$, 0.079 ± 0.001; and CD8$^+$ 0.028 ± 0.003 [(reference 2]); and OVA-treated sPLA$_2$-X$^{-/-}$ mice (CD3$^+$, 0.264 ± 0.051; CD4$^+$, 0.196 ± 0.025; and CD8$^+$, 0.065 ± 0.005 [reference 3]). *, $P < 0.05$ for both saline versus OVA in +/+ mice and OVA in +/+ mice versus OVA in −/− mice. (c) IL-1β, IL-2, IL-4, IL-5, IL-12α, IL-12β, IL-13, and IFN-γ mRNAs were determined by RT-PCR in whole-lung tissue from sPLA$_2$-X$^{+/+}$ and sPLA$_2$-X$^{-/-}$ mice on day 76. (d) IL-4, IL-5, and IL-13 protein levels (pg/ml) were determined in the BAL fluid obtained on day 76 in saline- and OVA-treated sPLA$_2$-X$^{+/+}$ (+/+) and sPLA$_2$-X$^{-/-}$ mice (−/−). *, $P < 0.05$ for both saline versus OVA in +/+ mice and OVA in +/+ mice versus OVA in −/− mice. Data represent the mean ± SEM.

model, PGD_2 (Fig. 9 a), PGE_2 (Fig. 9 b), LTB_4 (Fig. 9 c), and cysLT (Fig. 9 d) levels were each significantly increased in the BAL fluid of sPLA$_2$-X$^{+/+}$ mice after OVA treatment compared with saline controls with cysLTs>>PGE_2>LTB_4>PGD_2. The 13,14-dihydro-15-keto-PGE_2 metabolite represented 91% of total PGE_2 levels in the OVA-treated wild-type mice. As determined by liquid chromatography–electrospray tandem mass spectrometry, the fractional distribution of LTC_4, LTD_4, and LTE_4 was similar in the BAL fluid of OVA- and saline-treated wild-type mice, with LTE_4 the predominant cysLT recovered (i.e., the respective fractional distributions of LTC_4:LTD_4:LTE_4 in OVA- and saline-treated sPLA$_2$-X$^{+/+}$ mice were 0.11:0.26:0.63 and 0.10:0.25:0.65, respectively). The levels of PGD_2, PGE_2, LTB_4, and cysLTs in the BAL fluid of allergen-challenged sPLA$_2$-X$^{-/-}$ mice were not significantly different than those of saline-controls (Fig. 9, a–d). The fractional distribution of LTC_4, LTD_4, and LTE_4 in the BAL fluid of OVA- and saline-treated sPLA$_2$-X$^{-/-}$ mice was the same as that observed for wild-type controls (0.11:0.26:0.63 for OVA-treated sPLA$_2$-X$^{-/-}$ mice and 0.10:0.25:0.65 for saline-treated sPLA$_2$-X$^{-/-}$ mice). On day 76 compared with saline controls (chronic model), both cyclooxygenase (i.e., PGE_2) and 5-lipoxygenase (i.e., cysLTs) products of arachidonic acid were substantially increased in the BAL fluid of wild-type but not sPLA$_2$-X$^{-/-}$ mice after OVA treatment (unpublished data).

DISCUSSION

Our results suggest that sPLA$_2$-X plays a critical role in the pathogenesis of the asthma phenotype. The major findings of this study are that deficiency of sPLA$_2$-X in mice substantially reduces allergen-induced (a) airway eosinophil and CD4$^+$ and CD8$^+$ T cell trafficking, mucus hypersecretion, and hyperresponsiveness to methacholine in an acute model of asthma; (b) airway remodeling (i.e., goblet cell metaplasia, smooth muscle cell layer thickening, and subepithelial fibrosis in the lungs) in a chronic asthma model; and (c) Th2 cytokine and eicosanoid levels in these models of human asthma.

Our data suggest that sPLA$_2$-X plays a role in eicosanoid generation and that the reduction in eicosanoid generation seen in the sPLA$_2$-X$^{-/-}$ mice leads to a decrease in Th2 responses. The Th2 cell subset of CD4$^+$ T cells has been recognized as pivotal in the development of this allergen-induced airway eosinophilic infiltration, mucus hypersecretion, fibrosis, and hyperreactivity through the secretion of IL-4, IL-5, and IL-13 cytokines. More recently, CD8$^+$ T cells have been demonstrated to substantially contribute to these allergen-induced responses by their trafficking to the lungs and local generation of IL-13 (29). We found that sPLA$_2$-X deficiency

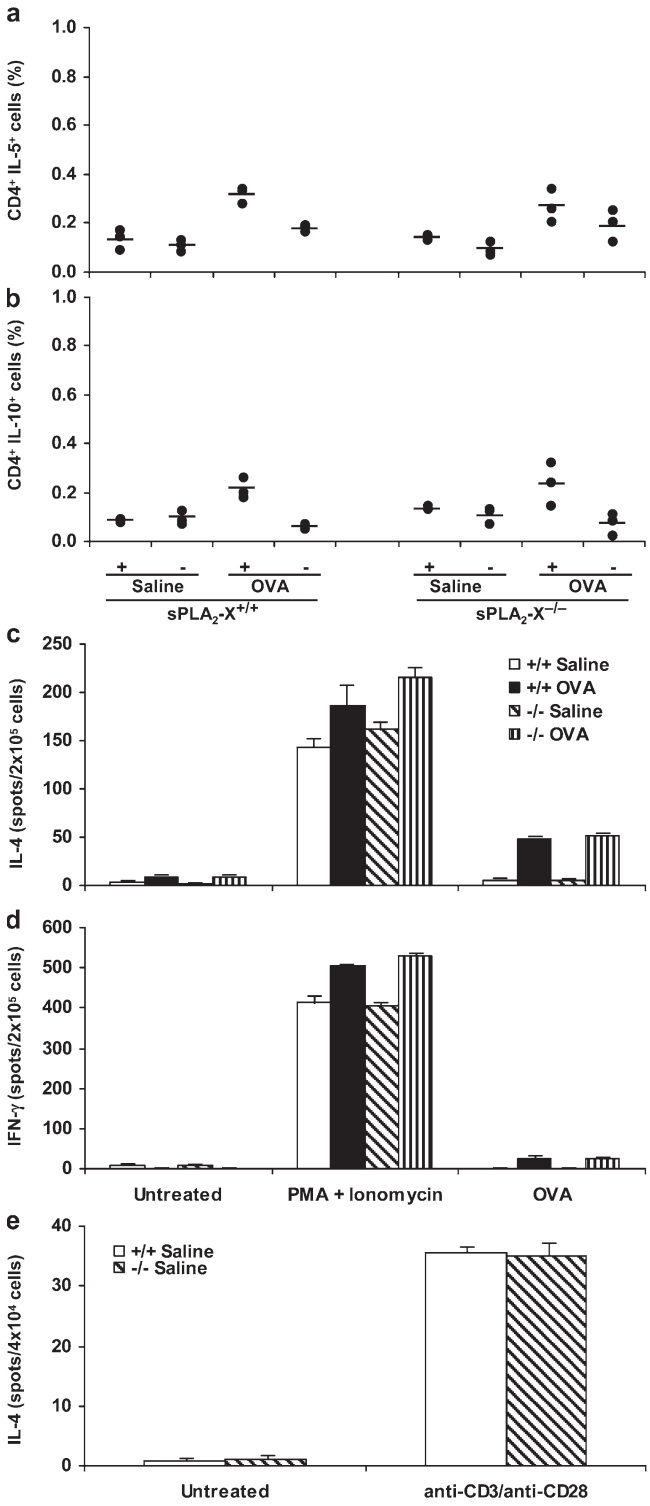

Figure 8. $sPLA_2$-X deficiency does not affect cytokine production in $CD4^+$ T cells. For flow cytrometric analysis of intracellular cytokines, splenocytes from saline- and OVA-treated $sPLA_2$-$X^{-/-}$ and $sPLA_2$-$X^{+/+}$ mice were cultured with or without 200 μg/ml OVA in the presence of antigen-presenting cells and stained for surface CD4 and the cytokines IL-5 (a) and IL-10 (b). The percentage of cytokine-producing $CD4^+$ cells from individual animals is shown. Horizontal bars represent the mean for three different age- and sex-matched animals. + represents cells activated in vitro with OVA, and − represents control cells incubated with PBS. For ELISPOT assay of IL-4 (c and e) and IFN-γ (d) production, splenocytes from $sPLA_2$-$X^{+/+}$ mice treated with saline (+/+) or OVA (+/+) and $sPLA_2$-$X^{-/-}$ mice treated with saline (−/−) or OVA (−/−) were incubated in the absence (untreated) or presence of either 5 ng/ml PMA/500 ng/ml ionomycin (PMA + ionomycin) or 500 μg/ml OVA (c and d), or $CD4^+$ cells isolated from the total splenic cells were incubated in the absence (untreated) or presence of anti-CD3/anti-CD28 antibodies (e). Data represent the mean ± SEM.

resulted in a marked decrease in movement of both $CD4^+$ and $CD8^+$ T cells to the airway lumen that was associated with diminished pulmonary Th2 cytokine gene and protein expression. Splenic T cells from the $sPLA_2$-$X^{-/-}$ mice showed normal induction of Th2 and Th1 cytokines with ex vivo stimulation. Thus, the marked impairment in the ability of the mutant mice to recruit allergen-specific T cells to the lungs likely accounts for the observed diminution in pulmonary Th2 cytokine production and inflammation. Among other key effects on the asthma phenotype, IL-13 induces secretion of mucin 5AC glycoprotein, differentiation of ciliated epithelial cells into goblet cells (30), and release of TGFβ, leading to fibrosis (31) in the airways of mice after allergen challenge. IL-4, in the absence of other Th2 cytokines, can also induce typical Th2 responses, including airway goblet cell metaplasia, in a mouse asthma model (32). IL-5 promotes growth and maturation of eosinophil precursors and stimulates the chemotaxis of mature eosinophils, prolonging their survival in allergic inflammatory tissue sites by inhibition of apoptosis (2). In both wild-type and $sPLA_2$-deficient mice, Th1 cytokines remained low after OVA stimulation.

We found that in $sPLA_2$-X–deficient mice, there is a reduction in elevated levels of eicosanoids found in OVA-treated wild-type mice, and this likely leads to an amelioration of the asthma phenotype. In mouse models of asthma, specific inhibitors of 5-lipoxygenase, or leukotriene receptor antagonists, considerably reduce indices of allergic airway inflammation, including Th2 cytokine levels (3, 4). The $cysLT_1$ receptor antagonist montelukast inhibits Th2 cytokine gene and protein expression in the lungs of sensitized mice chronically challenged with OVA (4). Further, established and persistent airway eosinophilia, goblet cell metaplasia, increased airway smooth muscle mass, and subepithelial fibrosis in a mouse model of allergen-induced airway remodeling are reversible by $cysLT_1$ receptor blockade (26). The cysLTs promote growth of eosinophil progenitors from the blood and bone marrow of atopic individuals (33), stimulate eosinophil chemotaxis, and increase their survival in tissue sites of allergic inflammation. Bronchial smooth muscle cells, with increased $cysLT_1$ receptor expression after TGFβ and IL-13 treatment, proliferate in response to LTD_4 (34). cysLTs also induce the release of mucus by airway goblet cells (3) and collagen by TGFβ-transformed lung myofibroblasts (35). In IL-13–induced airway inflammation and remodeling in mice, 5-lipoxygenase inhibitors, as well as $cysLT_1$ and LTB_4

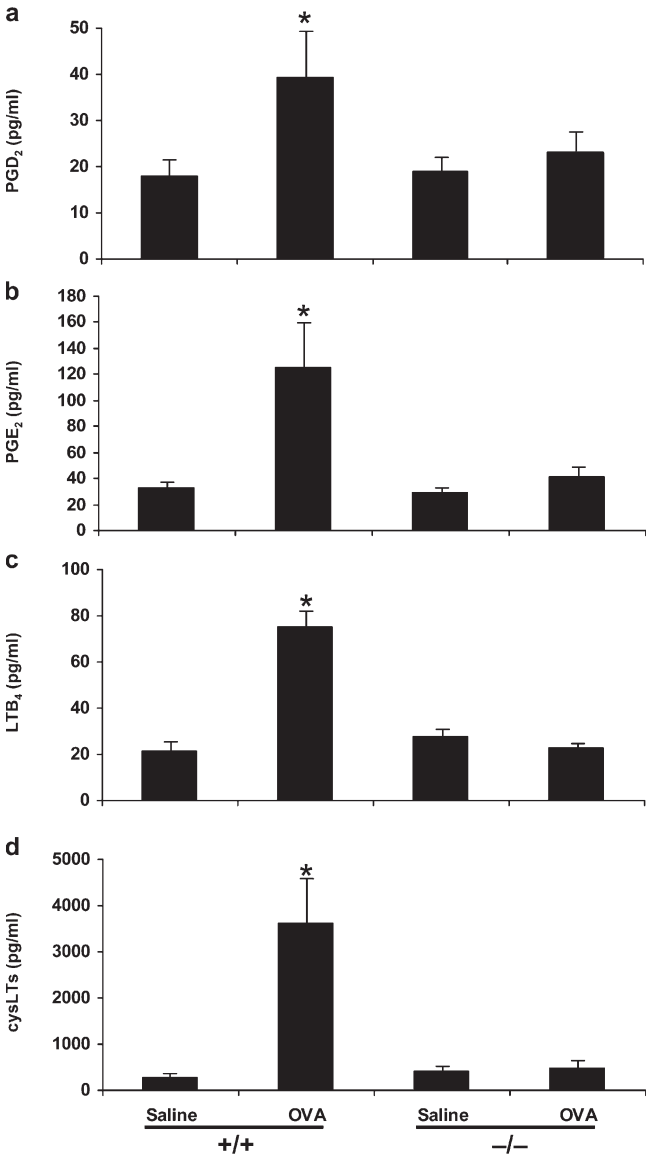

Figure 9. Impaired eicosanoid release in sPLA$_2$-X$^{-/-}$ mice. (a) PGD_2 (PGD_2-MOX), (b) PGE_2 (PGE_2 + 13,14,dihydro-15-keto-PGE_2 metabolite), (c) LTB_4, and (d) total cysLT levels were determined in BAL fluid obtained 1 h after the last aerosol OVA challenge on day 23 (acute asthma model) from saline- and OVA-treated sPLA$_2$-X$^{+/+}$ (+/+) and sPLA$_2$-X$^{-/-}$ (−/−) mice. Data represent the mean ± SEM. *, $P < 0.05$ versus other groups.

receptor antagonists, reduce eosinophil infiltration, mucus cell metaplasia, and collagen deposition in the airways, indicating that both LTB_4 and cysLTs C_4, D_4, and E_4 substantially contribute to the effects of IL-13 on the lung (5).

Recent studies have indicated an important role for LTB_4 and PGD_2 in directing T cells to the airways in asthma. Using mice deficient in the LTB_4 receptor BLT1, a requirement of the LTB_4–BLT1 pathway, has been demonstrated as crucial for the early recruitment of $CD4^+$ and $CD8^+$ T cells to the airways after allergen challenge (36). The T cell–mediated allergen-induced airway hyperresponsiveness in this model is dependent on BLT1 and is associated with IL-13 production by the T cells (37, 38). Increased numbers of $BLT1^+$ T cells are found in the airways of allergic individuals with asthma (39). Mice deficient in DP_1, one of the receptors for PGD_2, have decreased airway Th2 cytokines, eosinophil infiltration, and mucus hypersecretion compared with wild-type controls after allergen sensitization and challenge (40). PGD_2 induces preferential generation of Th2 cytokines by its interaction with the chemoattractant receptor–like molecule expressed on Th2 cells (41).

Over the past decade, it has generally been considered that cPLA$_2$-α is the master regulator of arachidonate release from cellular phospholipids. Early reports showed that group IIA sPLA$_2$ (*PLA2G2A*) rises to high levels in serum and synovial fluid in patients suffering from inflammatory disorders, including acute pancreatitis and rheumatoid arthritis (42, 43), but there was no evidence showing that group IIA sPLA$_2$ is directly responsible for the liberation of arachidonate from phospholipids for the biosynthesis of eicosanoids. More recent work has shown that sPLA$_2$s can augment the action of cPLA$_2$-α in cells to liberate arachidonate. Peritoneal macrophages from group V sPLA$_2$-deficient mice produce ∼50% as much free arachidonate compared with wild-type cells after stimulation with zymosan, a fungal cell wall–derived agonist (14), yet there is essentially no arachidonate released in this system when macrophages from cPLA$_2$-α–deficient mice are used (13). Earlier studies with antisense technology to knock down the level of group V sPLA$_2$ also support a role for a joint action of group V sPLA$_2$ and cPLA$_2$-α in macrophages (16). Thus, cPLA$_2$-α and group V sPLA$_2$ work together by an unknown mechanism leading to maximal arachidonate release. Because both enzymes are PLA$_2$s that can hydrolyze arachidonyl-containing phospholipids, it is not possible at this point to know which enzyme is directly responsible for most of the phospholipid *sn*-2 lipolysis leading to arachidonate release.

In rat gastric epithelial cells (RGM1) and in rat fibroblasts (3Y1), cytokine-induced arachidonate release and PGE_2 production coincide with up-regulation and secretion of group IIA sPLA$_2$ into the culture medium, and studies with cPLA$_2$-α and sPLA$_2$ inhibitors support a coordinate role for both enzymes in arachidonate release (15, 17). Coordinate action of cPLA$_2$-α and sPLA$_2$s has also been recently reported in transfected cells (18, 19). There are no reports showing that endogenous sPLA$_2$-X is directly involved in arachidonic acid release from mammalian cells in culture. Nevertheless, we decided to explore the sPLA$_2$-X$^{-/-}$ mouse in an animal model of asthma because of the high activity that this enzyme shows when added to mammalian cells in culture (21, 22). The results of the present study showing a clear role for sPLA$_2$-X in mediating airway inflammation in a mouse model of allergic asthma are thus important and novel. Our study is the first to demonstrate an important role for an sPLA$_2$ in an animal model of asthma. It remains to be seen if other mammalian sPLA$_2$s play a role in airway inflammation and hyperreactivity.

In OVA-treated wild-type mice, a strong signal in immunohistochemical detection of $sPLA_2$-X in mouse lung sections was seen in airway epithelial cells and alveolar macrophages. $sPLA_2$-X colocalized with airway epithelial cells expressing mucin 5AC, a major gel-forming mucin of mouse (44) and human (45) airway epithelial cells. Studies using in situ hybridization for mRNA detection have shown that human lung epithelial cells also express $sPLA_2$-X, along with $sPLA_2$-V (24). It is generally thought that airway epithelial cells lack the lipoxygenases and cyclooxygenases needed to convert free arachidonate into leukotrienes and prostaglandins. However, in vitro cell co-culture studies have shown that arachidonate released from stimulated airway epithelial cells can be transferred to nearby macrophages and eosinophils for oxygenation leading to eicosanoids (46, 47). Thus, a reasonable working hypothesis for the results seen in the current study is that airway epithelial cell $sPLA_2$-X generates free arachidonate, which is converted into proinflammatory eicosanoids by nearby leukocytes. Studies are underway to test this hypothesis by selectively disrupting the $sPLA_2$-X gene in airway epithelial cells.

Our data demonstrating a profound effect of $sPLA_2$-X deficiency on Th2 cell–driven airway inflammation and remodeling in a mouse model of human asthma bring a new dimension to the PLA_2 field. These findings point to $sPLA_2$-X as a potential target for the development of novel anti-asthma drugs.

MATERIALS AND METHODS

Generation of the $sPLA_2$-X–deficient mouse. Embryonic stem cells ($129SvEv^{Brd}$-derived) containing a mutated $sPLA_2$-X gene were prepared by a high throughput gene trapping technique and used at Lexicon Genetics Inc. to generate a chimeric mouse in the $129SvEv^{Brd}$/C57BL/6J mixed background, as previously described (48, 49). This approach uses a multiplicity of infection with virus that disfavors multiple insertions of the trapping cassette. The $sPLA_2$-$X^{-/-}$ mouse was generated by breeding, and the genotype was verified by PCR using the primers LTR2, upper, and lower (primer sequences and PCR conditions are provided in Table S1, available at http://www.jem.org/cgi/content/full/jem.20070029/DC1). LTR2 and lower give the mutant band of 320 bp, and upper and lower give the wild-type band of 392 bp. Two lines of evidence indicate that the trapping cassette is present as a single copy in the genome: (a) rapid amplification of cDNA ends sequencing on the 3′ fusion transcript revealed only a single sequence, and (b) quantitative PCR on the neomycin cassette demonstrated only a single copy in heterozygote mice.

Analysis of $sPLA_2$-X mRNA and protein. We used primers to exons 2 and 4 for PCR analysis of cDNA isolated from mouse tissues. Mouse testis was ground in RNA lysis buffer (600 μl/100 mg of tissue; Promega) on ice, and RNA was isolated from 175 μl of suspension using a kit (Z3100; Promega). A 5-μl aliquot of the resultant 100 of RNA solution in water was converted to 20 μl of cDNA solution using a kit (Marligen Biosciences, Inc.). 1 μl of cDNA was used in a 25-μl PCR reaction with primers directed at the mouse glyceraldehyde-3–phosphate dehydrogenase mRNA sequence and predicted to form a 500-bp product spanning more than one exon. From the results of agarose gel electrophoresis on 5 μl of the PCR product after 23, 27, and 31 cycles of PCR, the amount of cDNA required just to show a perceptible band at 500 bp after 23 cycles was estimated. This amount was used in a second PCR reaction with the primers $sPLA_2$-X–F4 (from exon 2) and $sPLA_2$-X–RC (from exon 4). These primers gave an $sPLA_2$-X band of the correct size (480 bp) on a 2% agarose gel after 27 cycles of PCR with cDNA derived from testis from a $sPLA_2$-$X^{+/+}$ mouse, whereas 39 cycles of PCR were required to see this same band from the same amount of cDNA derived from testis from the $sPLA_2$-$X^{-/-}$ mouse, corresponding to ~1,000-fold reduction in $sPLA_2$-X mRNA. No PCR band was seen in a blank control after 39 PCR cycles.

To examine $sPLA_2$-X protein expression, stomachs from $sPLA_2$-$X^{-/-}$ and $sPLA_2$-$X^{+/+}$ littermate mice were flash frozen in liquid nitrogen and lyophilized. Each stomach was soaked in 200 μl of saline, mixed by vortexing, and incubated at 4°C for 30 min. Samples were centrifuged at 16,000 *g* for 10 min, and the supernatants were assayed for protein by the Bradford assay and for $sPLA_2$-X using time-resolved immunoassay, as previously described (25).

Allergen challenge in mice. All animal use procedures were approved by the University of Washington Animal Care Committee. $sPLA_2$-$X^{-/-}$ C57BL/129 mice and their wild-type $sPLA_2$-$X^{+/+}$ littermates received i.p. injections of 100 μg OVA (0.2 ml of 0.5 mg/ml; Pierce Chemical Co.) complexed with aluminum potassium sulfate (alum; Sigma-Aldrich) on days 0 and 14. Mice were anesthetized i.p. with 130 mg/kg ketamine and 8.8 mg/kg xylazine in normal saline before receiving an i.n. dose of 100 μg OVA (0.05 ml of 2 mg/ml) on day 14, and 50 μg OVA (0.05 ml of 1 mg/ml) on days 26, 27, and 28 (acute asthma model) or days 26, 27, 28, 47, 61, 73, 74, and 75 (chronic asthma model). Control groups received 0.2 ml of normal saline with alum i.p. on days 0 and 14, and 0.05 ml of saline without alum i.n. on days 14, 26, 27, and 28 or days 14, 26, 27, 28, 47, 61, 73, 74, and 75. Mouse plasma samples were obtained on day 29 from the OVA- and saline-treated groups and assayed for OVA-specific IgE (50). For eicosanoid analysis studies, mice were immunized i.p. with 10 μg OVA and 1.125 mg alum in 0.2 ml of normal saline on days 0, 7, and 14 and exposed to 1% aerosolized OVA, as previously described by Myou et al. (51) for 40 min on days 21, 22, and 23. Control groups received 0.2 ml of normal saline with alum i.p. on days 0, 7, and 14, and saline by aerosol on days 21, 22, and 23.

Pulmonary function testing. On day 29, invasive pulmonary mechanics were measured in mice in response to methacholine in the same manner as previously described (3), with the following modifications: (a) the thorax was not opened; (b) mice were ventilated with a tidal volume of 200 μl and a respiratory rate of 120 breaths per minute using a MiniVent Ventilator for Mice (Harvard Apparatus); (c) mice received aerosolized solutions of methacholine (0, 3.125, 6.25, 12.5, 25, and 50 mg/ml in normal saline) via a nebulizer aerosol system (AER 1021; Buxco Electronics) with a 2.5–4-μm aerosol particle size generated by a nebulizer head (NEB0126; Nektar Therapeutics); and (d) a commercial plethysmography system consisting of a plethysmograph (model PLY4111), amplifier and pressure transducer system (MAX II), and Biosystem XA software (all obtained from Buxco Electronics) was used to determine R_L as calculated from the measures of pressure and flow and expressed as cm H_2O/ml/s. Noninvasive plethysmography was also assessed on day 29, as described in Supplemental materials and methods (available at http://www.jem.org/cgi/content/full/jem.20070029/DC1).

BAL. After tying off the left lung at the mainstem bronchus, the right lung was lavaged three times with 0.5 ml of normal saline either 1 h (for eicosanoid assays) or 24 h (for cytokine assays) after the final OVA or saline treatment. The BAL fluid was centrifuged at 250 *g*, and the supernatant was processed for eicosanoid assays, as described in detail in Supplemental materials and methods. Total BAL fluid cells were counted with eosinophils stained with 0.05% eosin (3), and the number of $CD3^+$, $CD4^+$, and $CD8^+$ T cells was determined by cytofluorimetry. On day 29, alveolar macrophages were isolated from the BAL fluid cells by adherence to Esco Fluro slides (Erie Scientific Company) for 2 h in RPMI 1640 with L-glutamate (Cellgro; Mediatech, Inc.) in humidified 5% CO_2/95% air at 37°C, as previously described (52). To remove nonadherent cells, the slides were washed six times in PBS, and adherent cells were stained for $sPLA_2$-X expression.

Cytofluorimetry. BAL fluid cells were preincubated with 1 μg Fc Block (anti–mouse CD16/CD32 [FcγIII/II receptor]; BD Biosciences) per 10^6 cells in 50 μl of staining buffer (BD Biosciences) for 15 min at 4°C to reduce nonspecific immunostaining. After washing in PBS containing 1% FBS, pH 7.4 (Sigma-Aldrich), ~10^6 cells were incubated with 50 μl PBS + 1% FBS buffer containing 1 μg each of the following antibodies purchased from BD Biosciences: PE–anti–mouse CD3e (CD3ε chain; 145-2C11), allophycocyanin –anti–mouse CD4 (L3T4; RM4-5), and FITC–anti–mouse CD8a (Ly-2; 53-6.7) for 20 min at 4°C. Cells were fixed in 1% paraformaldehyde in PBS for 16 h at 4°C, and cytofluorimetry was performed with a flow cytometry system (Cytomics FC500; Beckman Coulter).

RT-PCR. Total RNA was isolated from the right lung using an RNeasy mini kit (QIAGEN), and mRNA levels for IL-1β, IL-2, IL-4, IL-5, IL-12α (IL-12 p35 subunit), IL-12β (IL-12 p40 subunit), IL-13, IFN-γ, and GAPDH were determined by RT-PCR. A PCR System (7900HT Fast Real-Time; Applied Biosystems) was used, and SYBR green PCR master mix was used (Applied Biosystems. 0.2 μg RNA was used to synthesize first-strand cDNA with the first-strand synthesis system (SuperScript III; Invitrogen). All primers were designed using primer 3 and crossed large expanses of the intronic sequence (Table S1). PCR sizes were ~100 bp and were confirmed by gel electrophoresis. RT-PCR readings had to be within the range of the standard curve. Sample cDNAs were diluted to 20 ng/μl.

Lung and spleen histopathology. The trachea, upper and lower lobes of the left lung, and spleen were fixed for 24 h in 10% neutral buffered formalin solution. The tissues were embedded in paraffin and cut into 5-μm sections. For lung morphometry, 10 airways (0.4–0.7 mm in diameter and surrounded by smooth muscle cells) per mouse were randomly selected and examined by individuals blinded to the protocol design (3). The sections were stained with hematoxylin and eosin to evaluate airway edema (i.e., alveolar flooding by amorphous material) on a semiquantitative 0–4+ scale (0 = 0–10% alveoli with edema; 1 = 10–20% alveoli with edema; 2 = 20–30% alveoli with edema; 3 = 30–40% alveoli with edema; and 4 = 40–50% alveoli with edema) (50) and total inflammatory cell infiltration (3) on a semiquantitative scale ranging from 0–4+ and eosinophil numbers per unit of lung tissue area (2,200 μm^2). Each field, at magnification of 400 using a micrometer disc (Whipple; Bausch & Lomb), represented 2,200 μm^2 of tissue area. The smooth muscle mass of the smooth muscle cell layer beneath the airway epithelial cell basement membrane was assessed on a 0–4+ scale at three sites tangential to each airway cross-section examined (4). The sections were stained with alcian blue/periodic acid Schiff (PAS) reaction to identify airway goblet cells and mucus (3). The number of goblet cells was determined as the percentage of total airway epithelial cells in each airway examined. Mucus occlusion of the airway diameter was assessed on a 0–4+ scale. Each airway section was assigned a score for airway diameter occlusion by mucus based on the following criteria: 0 = 0–10% occlusion; 1 = 10–30% occlusion; 2 = 30–60% occlusion; 3 = 60–90% occlusion; and 4 = 90–100% occlusion (3). To determine subepithelial collagen deposition/fibrosis in the airways, the sections were stained with Masson's trichrome stain (4). The intensity of the collagen deposition (0–4+ scale) was assessed in the immediate region beneath the epithelium containing the contractile elements and extracellular matrix associated with the airways, as described by Leigh et al. (53)

Immunocytochemistry. $sPLA_2$-X expression in mouse lung and spleen was localized by immunocytochemistry using light microscopy (54). Tissues were fixed in methyl Carnoy's solution and embedded in paraffin, and 5-μm sections were cut, placed on slides (Super Frost Plus;VWR Scientific), deparaffinized, hydrated, and rinsed in PBS. All immunolabeling procedures were performed at 24°C. Endogenous peroxidase was inactivated by incubating the tissue sections in 0.75% hydrogen peroxide for 30 min. After rinsing in PBS, the sections were incubated with the primary antibody, polyclonal rabbit anti–$sPLA_2$-X–specific antisera (55), at a 1:50 dilution for 25 min, followed by rinsing in PBS and incubation with the secondary antibody, goat anti–rabbit antibody conjugated to horseradish peroxidase (Vector Laboratories), at a 1:20 dilution for 25 min. The controls were either PBS or normal rabbit IgG (Vector Laboratories) used in place of the primary antibody. After rinsing in PBS, the sections were incubated with 0.5% 3′,3′-diaminobenzidine tetrachloride (Sigma-Aldrich) in PBS and 0.15% hydrogen peroxide for 15 min for detection of peroxidase. The sections were rinsed in PBS, and nuclei were counterstained with 1% methyl green in distilled water for 3 min. The sections were dehydrated in ethanol, cleared in xylene, and mounted on glass slides with Permount (Fisher Scientific). BAL fluid alveolar macrophages, isolated by overnight adherence to microscope slides, were also stained for $sPLA_2$-X by immunocytochemistry.

Immunofluorescence confocal microscopy. For immunofluorescence double staining of mucin 5AC and $sPLA_2$-X, lung tissue was frozen in liquid nitrogen immediately after collection, embedded in OCT compound (Tissue-Tek; Sakura Finetek USA, Inc.), and cut into 10-μm-thick cryostat sections. After rinsing in PBS, the slides were fixed in acetone for 5 min, washed three times in PBS, and blocked in 2% dry milk for 30 min at room temperature. The sections were incubated with the primary antibodies (both at a dilution of 1:100 in PBS), rabbit anti–mouse $sPLA_2$-X (55) and goat anti–mouse mucin 5AC (K-20; Santa Cruz Biotechnology, Inc.), for 40 min at room temperature, washed three times in PBS, and incubated with the secondary antibodies (both at a dilution of 1:100 in PBS; Invitrogen), Alexa Fluor 594 (i.e., red fluorophore) donkey anti–rabbit IgG and Alexa Fluor 488 (i.e., green fluorophore) donkey anti–goat IgG, for 30 min at room temperature. After washing in PBS, coverslips were placed with IMMU-MOUNT (Shandon Inc.), and slides were stored in the dark at 4°C. Sections were examined on a confocal microscope (LSM510Meta; Carl Zeiss MicroImaging, Inc.) running software version 4.0. Fluorescence excitation was provided using an argon laser line (488 nm) and a helium–neon laser line (543 nm).

Cytokine and eicosanoid analyses. Lincoplex multiplexed biomarker immunoassays of BAL fluid for IL-1β, IL-2, IL-4, IL-5, IL-12 (p70), and IFN-γ were performed using Luminex instrumentation (3.2 pg/ml detection limit; LINCO Research) according to the manufacturer's instructions. IL-13 (1.5 pg/ml detection limit; R&D Systems), LTB_4 (13 pg/ml detection limit; Cayman Chemical), cysLTs (LTC_4/LTD_4/LTE_4, 13 pg/ml detection limit; Cayman Chemical), PGD_2 (measured as the stable MOX derivative PGD_2-MOX after treatment of the samples with methoxylamine hydrochloride; 3.1 pg/ml detection limit using a PGD_2-MOX enzyme immunoassay (EIA) kit; Cayman Chemical), and PGE_2 (measured as the total of PGE_2 [15 pg/ml detection limit using a PGE_2 kit–monoclonal; Cayman Chemical] and its 13,14,dihydro-15-keto metabolite [2 pg/ml detection limit using a PGE_2 metabolite EIA kit; Cayman Chemical]) were determined by EIA. The fraction of cysLTs that are LTC_4, LTD_4, and LTE_4, was determined by combined liquid chromatography–electrospray tandem mass spectrometry using a modification of the method of Kita et al. (56). Full details of eicosanoid analyses are provided in Supplemental materials and methods.

For flow cytrometric analysis of intracellular cytokines, total splenic cell populations from experimental and control mice were plated in 24-well plates (4×10^6 cells per well) and activated with 200 μg/ml OVA (Pierce Chemical Co.) overnight. The samples were stained with pericinin-chlorophyll-*a*-protein–conjugated anti-CD4, allophycocyanin-conjugated anti-CD8, and PE-conjugated antibodies against the following cytokines: IL-4, IL-5, IL-10, TNF-α, and IFN-γ (antibodies were obtained from BD Biosciences and eBioscience). The intracellular staining for cytokines was performed using the manufacturer's standard protocol (BD Biosciences). Samples were analyzed using a flow cytometer (FACSCanto; BD Biosciences), and the data were analyzed using FlowJo software (TreeStar Inc.).

For enzyme-linked IL-4 and IFN-γ immunospot (ELISPOT) assays (BD Biosciences), total spleen cells from OVA- and saline-treated $sPLA_2$-$X^{-/-}$ mice and wild-type controls were collected, plated in 96-well plates (2×10^5 cells/well), and incubated in triplicate in 5% CO_2/95% air at 37°C in the absence or presence of 5 ng/ml PMA (Sigma-Aldrich) and 500 ng/ml ionomycin (Sigma-Aldrich) for 24 h or 500 μg/ml OVA (Pierce Chemical Co.) for

5 d according to the manufacturer's protocol (BD Biosciences). $CD4^+$ T cells were isolated from the spleen cells using Dynabeads Mouse CD4 (L3T4) and DETACHsBEAD Mouse CD4 (Dynal), according to the manufacturer's instructions. 4×10^4 $CD4^+$ T cells/well were incubated in triplicate in 5% CO_2/95% air at 37°C in the absence or presence of 1 μg/ml of hamster anti–mouse CD3ε/2 μg/ml of hamster anti–mouse CD28 monoclonal antibodies (BD Biosciences) for 5 d, and IL-4 immunospot was performed.

Statistical analysis. Data are reported as the mean ± SEM. Differences were analyzed for significance ($P < 0.05$) by analysis of variance using the least significant difference method.

Online supplemental material. Fig. S1 shows $sPLA_2$-X expression in airway cells of OVA-treated $sPLA_2$-$X^{+/+}$ mice by immunocytochemistry. Fig. S2 shows that $sPLA_2$-X expression is seen in splenic mononuclear cells in $sPLA_2$-$X^{+/+}$ mice but is absent in $sPLA_2$-$X^{-/-}$ mice by immunocytochemistry. Fig. S3 shows decreased goblet cell metaplasia and mucus release in the lungs of $sPLA_2$-$X^{-/-}$ mice after allergen challenge in an acute asthma model. Fig. S4 shows reduced levels of eosinophils in BAL fluid of OVA-treated $sPLA_2$-$X^{-/-}$ mice in a chronic asthma model. Fig. S5 shows reduced allergen-induced airway inflammatory cell infiltration and edema in $sPLA_2$-$X^{-/-}$ mice in a chronic asthma model. Table S1 provides the sequence of PCR primers and PCR conditions used. Supplemental materials and methods contains details of the procedure for BAL fluid eicosanoid analysis by liquid chromatography–electrospray tandem mass spectrometry and EIA and pulmonary function testing by noninvasive plethysmography. Online supplemental material is available at http://www.jem.org/cgi/content/full/jem.20070029/DC1.

We thank Lexicon Genetics Inc. for generation of the $sPLA_2$-X–deficient mouse, Yoshihara Kita and Takao Shimizu and Nilda Muñoz for assistance with eicosanoid analysis, and Ronald Seifert for help with the confocal microscopy.

This work was funded by National Institutes of Health grants RO1 AI 42989 and HL 73722 (to W.R. Henderson Jr.) and HL 36235 (to M.H. Gelb).

The authors have no conflicting financial interests.

Submitted: 2 January 2007
Accepted: 1 March 2007

REFERENCES

1. Holgate, S.T. 1999. The epidemic of allergy and asthma. *Nature*. 402:B2–B4.
2. Kay, A.B. 2001. Allergy and allergic diseases. First of two parts. *N. Engl. J. Med.* 344:30–37.
3. Henderson, W.R., Jr., D.B. Lewis, R.K. Albert, Y. Zhang, W.J.E. Lamm, G.K.S. Chiang, F. Jones, P. Eriksen, Y. Tien, M. Jonas, and E.Y. Chi. 1996. The importance of leukotrienes in airway inflammation in a mouse model of asthma. *J. Exp. Med.* 184:1483–1494.
4. Henderson, W.R., Jr., L.-O. Tang, S.-J. Chu, S.-M. Tsao, G.K.S. Chiang, F. Jones, M. Jonas, C. Pae, H. Wang, and E.Y. Chi. 2002. A role for cysteinyl leukotrienes in airway remodeling in a mouse asthma model. *Am. J. Respir. Crit. Care Med.* 165:108–116.
5. Vargaftig, B.B., and M. Singer. 2003. Leukotrienes mediate murine bronchopulmonary hyperreactivity, inflammation, and part of mucosal metaplasia and tissue injury induced by recombinant murine interleukin-13. *Am. J. Respir. Cell Mol. Biol.* 28:410–419.
6. Valentin, E., and G. Lambeau. 2000. Increasing molecular diversity of secreted phospholipases A_2 and their receptors and binding proteins. *Biochim. Biophys. Acta.* 1488:59–70.
7. Bartoli, F., H.K. Lin, F. Ghomashchi, M.H. Gelb, M.K. Jain, and R. Apitz-Castro. 1994. Tight binding inhibitors of 85-kDa phospholipase A_2 but not 14-kDa phospholipase A_2 inhibit release of free arachidonate in thrombin-stimulated human platelets. *J. Biol. Chem.* 269:15625–15630.
8. Riendeau, D., J. Guay, P.K. Weech, F. Laliberte, J. Yergey, C. Li, S. Desmarais, H. Perrier, S. Liu, and D. Nicoll-Griffith. 1994. Arachidonyl trifluoromethyl ketone, a potent inhibitor of 85-kDa phospholipase A_2, blocks production of arachidonate and 12-hydroxyeicosatetraenoic acid by calcium ionophore-challenged platelets. *J. Biol. Chem.* 269:15619–15624.
9. Ghomashchi, F., A. Stewart, Y. Hefner, S. Ramanadham, J. Turk, C.C. Leslie, and M.H. Gelb. 2001. A pyrrolidine-based specific inhibitor of cytosolic phospholipase $A_2\alpha$ blocks arachidonic acid release in a variety of mammalian cells. *Biochim. Biophys. Acta.* 1513:160–166.
10. Rubin, B.B., G.P. Downey, A. Koh, N. Degousee, F. Ghomashchi, L. Nallan, E. Stefanski, D.W. Harkin, C. Sun, B.P. Smart, et al. 2005. Cytosolic phospholipase A_2-α is necessary for platelet-activating factor biosynthesis, efficient neutrophil-mediated bacterial killing, and the innate immune response to pulmonary infection: $cPLA_2\alpha$ does not regulate neutrophil NADPH oxidase activity. *J. Biol. Chem.* 280:7519–7529.
11. Uozumi, N., K. Kume, T. Nagase, N. Nakatani, S. Ishii, F. Tashiro, Y. Komagata, K. Maki, K. Ikuta, Y. Ouchi, et al. 1997. Role of cytosolic phospholipase A_2 in allergic response and parturition. *Nature.* 390:618–622.
12. Bonventre, J.V., Z. Huang, M.R. Taheri, E. O'Leary, E. Li, M.A. Moskowitz, and A. Sapirstein. 1997. Reduced fertility and postischaemic brain injury in mice deficient in cytosolic phospholipase A_2. *Nature.* 390:622–625.
13. Gijon, M.A., D.M. Spencer, A.R. Siddiqi, J.V. Bonventre, and C.C. Leslie. 2000. Cytosolic phospholipase A_2 is required for macrophage arachidonic acid release by agonists that do and do not mobilize calcium. Novel role of mitogen-activated protein kinase pathways in cytosolic phospholipase A_2 regulation. *J. Biol. Chem.* 275:20146–20156.
14. Satake, Y., B.L. Diaz, B. Balestrieri, B.K. Lam, Y. Kanaoka, M.J. Grusby, and J.P. Arm. 2004. Role of group V phospholipase A_2 in zymosan-induced eicosanoid generation and vascular permeability revealed by targeted gene disruption. *J. Biol. Chem.* 279:16488–16494.
15. Akiba, S., R. Hatazawa, K. Ono, K. Kitatani, M. Hayama, and T. Sato. 2001. Secretory phospholipase A_2 mediates cooperative prostaglandin generation by growth factor and cytokine independently of preceding cytosolic phospholipase A_2 expression in rat gastric epithelial cells. *J. Biol. Chem.* 276:21854–21862.
16. Balboa, M.A., J. Balsinde, M.V. Winstead, J.A. Tischfield, and E.A. Dennis. 1996. Novel group V phospholipase A_2 involved in arachidonic acid mobilization in murine P388D macrophages. *J. Biol. Chem.* 271:32381–32384.
17. Kuwata, H., T. Nonaka, M. Murakami, and I. Kudo. 2005. Search of factors that intermediate cytokine-induced group IIA phospholipase A_2 expression through the cytosolic phospholipase A_2- and 12/15-lipoxygenase-dependent pathway. *J. Biol. Chem.* 280:25830–25839.
18. Mounier, C.M., F. Ghomashchi, M.R. Lindsay, S. James, A.G. Singer, R.G. Parton, and M.H. Gelb. 2004. Arachidonic acid release from mammalian cells transfected with human groups IIA and X secreted phospholipase A_2 occurs predominantly during the secretory process and with the involvement of cytosolic phospholipase A_2-α. *J. Biol. Chem.* 279:25024–25038.
19. Han, W.K., A. Sapirstein, C.C. Hung, A. Alessandrini, and J.V. Bonventre. 2003. Cross-talk between cytosolic phospholipase $A_2\alpha$ ($cPLA_2\alpha$) and secretory phospholipase A_2 ($sPLA_2$) in hydrogen peroxide-induced arachidonic acid release in murine mesangial cells: $sPLA_2$ regulates $cPLA_2\alpha$ activity that is responsible for arachidonic acid release. *J. Biol. Chem.* 278:24153–24163.
20. Kim, Y.J., K.P. Kim, S.K. Han, N.M. Munoz, X. Zhu, H. Sano, A.R. Leff, and W. Cho. 2002. Group V phospholipase A_2 induces leukotriene biosynthesis in human neutrophils through the activation of group IVA phospholipase A_2. *J. Biol. Chem.* 277:36479–36488.
21. Singer, A.G., F. Ghomashchi, C. Le Calvez, J. Bollinger, S. Bezzine, M. Rouault, M. Sadilek, M. Lazdunski, G. Lambeau, and M.H. Gelb. 2002. Interfacial kinetic and binding properties of the complete set of human and mouse groups I, II, V, X, and XII secreted phospholipases A_2. *J. Biol. Chem.* 277:48535–48539.
22. Saiga, A., Y. Morioka, T. Ono, K. Nakano, Y. Ishimoto, H. Arita, and K. Hanasaki. 2001. Group X secretory phospholipase A_2 induces potent productions of various lipid mediators in mouse peritoneal macrophages. *Biochim. Biophys. Acta.* 1530:67–76.

23. Hanasaki, K., T. Ono, A. Saiga, Y. Morioka, M. Ikeda, K. Kawamoto, K. Higashino, K. Nakano, K. Yamada, J. Ishizaki, and H. Arita. 1999. Purified group X secretory phospholipase A_2 induced prominent release of arachidonic acid from human myeloid leukemia cells. *J. Biol. Chem.* 274:34203–34211.
24. Seeds, M.C., K.A. Jones, H.R. Duncan, M.C. Willingham, H.M. Borgerink, R.D. Woodruff, D.L. Bowton, and D.A. Bass. 2000. Cell-specific expression of group X and group V secretory phospholipases A_2 in human lung airway epithelial cells. *Am. J. Respir. Cell Mol. Biol.* 23:37–44.
25. Nevalainen, T.J., L.I. Eerola, E. Rintala, V.J. Laine, G. Lambeau, and M.H. Gelb. 2005. Time-resolved fluoroimmunoassays of the complete set of secreted phospholipases A_2 in human serum. *Biochim. Biophys. Acta.* 1733:210–223.
26. Henderson, W.R., Jr., G.K.S. Chiang, Y.T. Tien, and E.Y. Chi. 2006. Reversal of allergen-induced airway remodeling by $CysLT_1$ receptor blockade. *Am. J. Respir. Crit. Care Med.* 173:718–728.
27. Fitzpatrick, F.A., and M.A. Wynalda. 1983. Albumin-catalyzed metabolism of prostaglandin D_2. Identification of products formed in vitro. *J. Biol. Chem.* 258:11713–11718.
28. Hamberg, M., and B. Samuelsson. 1971. On the metabolism of prostaglandins E 1 and E 2 in man. *J. Biol. Chem.* 246:6713–6721.
29. Miyahara, N., B.J. Swanson, K. Takeda, C. Taube, S. Miyahara, T. Kodama, A. Dakhama, V.L. Ott, and E.W. Gelfand. 2004. Effector CD8+ T cells mediate inflammation and airway hyper-responsiveness. *Nat. Med.* 10:865–869.
30. Tyner, J.W., E.Y. Kim, K. Ide, M.R. Pelletier, W.T. Roswit, J.D. Morton, J.T. Battaile, A.C. Patel, G.A. Patterson, M. Castro, et al. 2006. Blocking airway mucous cell metaplasia by inhibiting EGFR antiapoptosis and IL-13 transdifferentiation signals. *J. Clin. Invest.* 116:309–321.
31. Lee, C.G., R.J. Homer, Z. Zhu, S. Lanone, X. Wang, V. Koteliansky, J.M. Shipley, P. Gotwals, P. Noble, Q. Chen, et al. 2001. Interleukin-13 induces tissue fibrosis by selectively stimulating and activating transforming growth factor β1. *J. Exp. Med.* 194:809–821.
32. Fallon, P.G., H.E. Jolin, P. Smith, C.L. Emson, M.J. Townsend, R. Fallon, P. Smith, and A.N. McKenzie. 2002. IL-4 induces characteristic Th2 responses even in the combined absence of IL-5, IL-9, and IL-13. *Immunity.* 17:7–17.
33. Braccioni, F., S.C. Dorman, P.M. O'Byrne, M.D. Inman, J.A. Denburg, K. Parameswaran, A.J. Baatjes, R. Foley, and G.M. Gauvreau. 2002. The effect of cysteinyl leukotrienes on growth of eosinophil progenitors from peripheral blood and bone marrow of atopic subjects. *J. Allergy Clin. Immunol.* 110:96–101.
34. Espinosa, K., Y. Bosse, J. Stankova, and M. Rola-Pleszczynski. 2003. $CysLT_1$ receptor upregulation by TGF-β and IL-13 is associated with bronchial smooth muscle cell proliferation in response to LTD_4. *J. Allergy Clin. Immunol.* 111:1032–1040.
35. Asakura, T., Y. Ishii, K. Chibana, and T. Fukuda. 2004. Leukotriene D_4 stimulates collagen production from myofibroblasts transformed by TGF-β. *J. Allergy Clin. Immunol.* 114:310–315.
36. Tager, A.M., S.K. Bromley, B.D. Medoff, S.A. Islam, S.D. Bercury, E.B. Friedrich, A.D. Carafone, R.E. Gerszten, and A.D. Luster. 2003. Leukotriene B_4 receptor BLT1 mediates early effector T cell recruitment. *Nat. Immunol.* 4:982–990.
37. Miyahara, N., K. Takeda, S. Miyahara, C. Taube, A. Joetham, T. Koya, S. Matsubara, A. Dakhama, A.M. Tager, A.D. Luster, and E.W. Gelfand. 2005. Leukotriene B_4 receptor-1 is essential for allergen-mediated recruitment of $CD8^+$ T cells and airway hyperresponsiveness. *J. Immunol.* 174:4979–4984.
38. Miyahara, N., K. Takeda, S. Miyahara, S. Matsubara, T. Koya, A. Joetham, E. Krishnan, A. Dakhama, B. Haribabu, and E.W. Gelfand. 2005. Requirement for leukotriene B_4 receptor 1 in allergen-induced airway hyperresponsiveness. *Am. J. Respir. Crit. Care Med.* 172:161–167.
39. Islam, S.A., S.Y. Thomas, C. Hess, B.D. Medoff, T.K. Means, C. Brander, C.M. Lilly, A.M. Tager, and A.D. Luster. 2006. The leukotriene B_4 lipid chemoattractant receptor BLT1 defines antigen-primed T-cells in humans. *Blood.* 107:444–453.
40. Matsuoka, T., M. Hirata, H. Tanaka, Y. Takahashi, T. Murata, K. Kabashima, Y. Sugimoto, T. Kobayashi, F. Ushikubi, Y. Aze, et al. 2000. Prostaglandin D_2 as a mediator of allergic asthma. *Science.* 287:2013–2017.
41. Xue, L., S.L. Gyles, F.R. Wettey, L. Gazi, E. Townsend, M.G. Hunter, and R. Pettipher. 2005. Prostaglandin D_2 causes preferential induction of proinflammatory Th2 cytokine production through an action on chemoattractant receptor-like molecule expressed on Th2 cells. *J. Immunol.* 175:6531–6536.
42. Nevalainen, T.J., J.M. Gronroos, and P.T. Kortesuo. 1993. Pancreatic and synovial type phospholipases A_2 in serum samples from patients with severe acute pancreatitis. *Gut.* 34:1133–1136.
43. Pruzanski, W., P. Vadas, E. Stefanski, and M.B. Urowitz. 1985. Phospholipase A_2 activity in sera and synovial fluids in rheumatoid arthritis and osteoarthritis. Its possible role as a proinflammatory enzyme. *J. Rheumatol.* 12:211–216.
44. Yu, M., M. Tsai, S.Y. Tam, C. Jones, J. Zehnder, and S.J. Galli. 2006. Mast cells can promote the development of multiple features of chronic asthma in mice. *J. Clin. Invest.* 116:1633–1641.
45. Kirkham, S., J.K. Sheehan, D. Knight, P.S. Richardson, and D.J. Thornton. 2002. Heterogeneity of airways mucus: variations in the amounts and glycoforms of the major oligomeric mucins MUC5AC and MUC5B. *Biochem. J.* 361:537–546.
46. Peters-Golden, M., and A. Feyssa. 1993. Transcellular eicosanoid synthesis in cocultures of alveolar epithelial cells and macrophages. *Am. J. Physiol.* 264:L438–L447.
47. Wijewickrama, G.T., J.-H. Kim, Y.J. Kim, A. Abraham, Y. Oh, B. Ananthanarayanan, M. Kwatia, S.J. Ackerman, and W. Cho. 2006. Systematic evaluation of transcellular activities of secretory phospholipases A_2. High activity of group V phospholipases A_2 to induce eicosanoid biosynthesis in neighboring inflammatory cells. *J. Biol. Chem.* 281:10935–10944.
48. Zambrowicz, B.P., G.A. Friedrich, E.C. Buxton, S.L. Lilleberg, C. Person, and A.T. Sands. 1998. Disruption and sequence identification of 2,000 genes in mouse embryonic stem cells. *Nature.* 392:608–611.
49. Zambrowicz, B.P., A. Abuin, R. Ramirez-Solis, L.J. Richter, J. Piggott, H. Beltrandel, E.C. Rio, J. Buxton, R.A. Edwards, C.J. Finch, et al. 2003. Wnk1 kinase deficiency lowers blood pressure in mice: a gene-trap screen to identify potential targets for therapeutic intervention. *Proc. Natl. Acad. Sci. USA.* 100:14109–14114.
50. Henderson, W.R., Jr., E.R. Banerjee, and E.Y. Chi. 2005. Differential effects of (S)- and (R)-enantiomers of albuterol in a mouse asthma model. *J. Allergy Clin. Immunol.* 116:332–340.
51. Myou, S., A.R. Leff, S. Myo, E. Boetticher, J. Tong, A.Y. Meliton, J. Liu, N.M. Munoz, and X. Zhu. 2003. Blockade of inflammation and airway hyperresponsiveness in immune-sensitized mice by dominant-negative phosphoinositide 3-kinase–TAT. *J. Exp. Med.* 198:1573–1582.
52. Neill, M.A., W.R. Henderson, and S.J. Klebanoff. 1985. Oxidative degradation of leukotriene C_4 by human monocytes and monocyte-derived macrophages. *J. Exp. Med.* 162:1634–1644.
53. Leigh, R., R. Ellis, J. Wattie, D.S. Southam, M. De Hoogh, J. Gauldie, P.M. O'Byrne, and M.D. Inman. 2002. Dysfunction and remodeling of the mouse airway persist after resolution of acute allergen-induced airway inflammation. *Am. J. Respir. Cell Mol. Biol.* 27:526–535.
54. Henderson, W.R., Jr., E.Y. Chi, R.K. Albert, S.-J. Chu, W.J.E. Lamm, Y. Rochon, P.E. Christie, and J.M. Harlan. 1997. Blockade of CD49d (α_4 integrin) on intrapulmonary but not circulating leukocytes inhibits airway inflammation and hyperresponsiveness in a mouse model of asthma. *J. Clin. Invest.* 100:3083–3092.
55. Degousee, N., F. Ghomashchi, E. Stefanski, A. Singer, B.P. Smart, N. Borregaard, R. Reithmeier, T.F. Lindsay, C. Lichtenberger, W. Reinisch, et al. 2002. Groups IV, V, and X phospholipases A_2s in human neutrophils: role in eicosanoid production and gram-negative bacterial phospholipid hydrolysis. *J. Biol. Chem.* 277:5061–5073.
56. Kita, Y., T. Takahashi, N. Uozumi, and T. Shimizu. 2005. A multiplex quantitation method for eicosanoids and platelet-activating factor using column-switching reversed-phase liquid chromatography-tandem mass spectrometry. *Anal. Biochem.* 342:134–143.